Astron. Astrophys. 320, 428–439 (1997)

ASTRONOMY AND ASTROPHYSICS

The evolution of the Milky Way disc

I. Vertical structure and local constraints

M. Haywood[1], **A.C. Robin**[2,3], **and M. Crézé**[3]

[1] DASGAL, URA CNRS 335, Section d'Astrophysique, Observatoire de Paris, F-92195 Meudon Cedex, France, (Misha.Haywood@obspm.fr)
[2] Observatoire de Besançon, 41 bis, Av. de l'Observatoire, BP 1615, F-25010 Besançon Cedex, France, (Robin@obs-besancon.fr)
[3] Observatoire de Strasbourg, CNRS URA 1280, 11 rue de l'Université, F-67000 Strasbourg, France, (Michel.Creze@iu-vannes.fr)

Received 5 April 1996 / Accepted 9 May 1996

Abstract. Deriving the Initial Mass Function and the Star Formation Rate (hereafter IMF and SFR) history of disc stars from local data implies assumptions concerning the vertical structure of the disc. Conversely, an accurate description of the vertical density of the stellar disc would require a precise knowledge of the stellar formation history. In this paper, the constraints available from local data on these two aspects are reviewed, and the interdependence between the SFR, the secular heating of the disc stars, and the shape of the density profile in the z direction is quantified.

As a consequence, the validity of exponential density models to represent the vertical structure of the disc is questioned and the uncertainties that affect the IMF derivation from the local LF are reevaluated. We show that under realistic assumptions on the SFR history, the observed local luminosity function gives little support for a bimodal IMF. Comparison of the observed local LF with synthetic LF brings tighter contraints on acceptable SFR and their corresponding IMF between 1 and 3 solar masses. These include decreasing SFR with IMF index x $\approx$1.5, constant SFR with IMF index x $\approx$2.0, or increasing SFR with IMF index x $\approx$2.5.

Key words: stars: luminosity function, mass function – Galaxy: evolution – Galaxy: solar neighbourhood – Galaxy: stellar content – Galaxy: structure

1. Introduction

The evolution of the galactic disc involves several time-dependent mechanisms which combination produces the present-day space-luminosity-velocity distribution : the heating rate of the disc, the star formation rate, and the initial distribution of stellar masses at different epochs. The luminosity function as it is observed in the solar neighbourhood result from the combination of these three processes. Due to the sparse nature of the available data for investigation of the IMF at masses greater than 1 $M_\odot$ in the solar neighbourhood, most investigations should rely upon assumptions concerning one or two of these processes, for which there exists, however, a rather weak observational or theoretical basis.

One of these assumptions, which is very efficient to work with, postulates that the distribution of stellar masses at birth has remained constant with time. This strong assumption has sometimes been alleviated with the bimodal hypotheses (Scalo (1986), Larson (1986)). From the observational point of view, a basic support for the bimodal hypotheses was the flattening or dip found in the observed luminosity function (hereafter LF) at M_v=6-9, which was interpreted by Scalo as being due to a corresponding feature in the IMF. This suggestion has been seriously questioned by D'Antona & Mazzitelli (1986), Kroupa, Tout & Gilmore (1990, 1991, 1993) (hereafter KTG (1990), etc), and Haywood (1994), all attributing this feature in the LF to the non-linear behavior of the mass-M_v relation. If the IMF in the corresponding mass range can be described by a single power law slope, one question nevertheless remains: Scalo gives evidence for a rise in the IMF at M>1 $M_\odot$, if a decreasing or constant star formation rate is assumed. As noted by Scalo, such a change in the IMF at exactly 1 $M_\odot$ is an embarrassing result, which can only be avoided by exploring the following alternatives: either this feature tells us that constant or decreasing SFR are an inadequate description of SFR history in the galactic disc, or we should consider that the derivation of the IMF contains various sources of error which have been underestimated.

The second most important assumption concerns the density decrease perpendicular to the galactic plane. This decrease is usually assumed exponential in determinations of the local IMF (Miller & Scalo (1979), Scalo (1986)) and in Galaxy models (Bahcall & Soneira (1981), Gilmore (1984) etc), with a scale height of 300-350 pc. Recent determinations of the scale height of the galactic disc stars in the solar neighbourhood (Soubiran (1994), KTG (1993), and Ojha (1994)) have a systematic discrepancy with these values. This problem is quite important

Send offprint requests to: M. Haywood

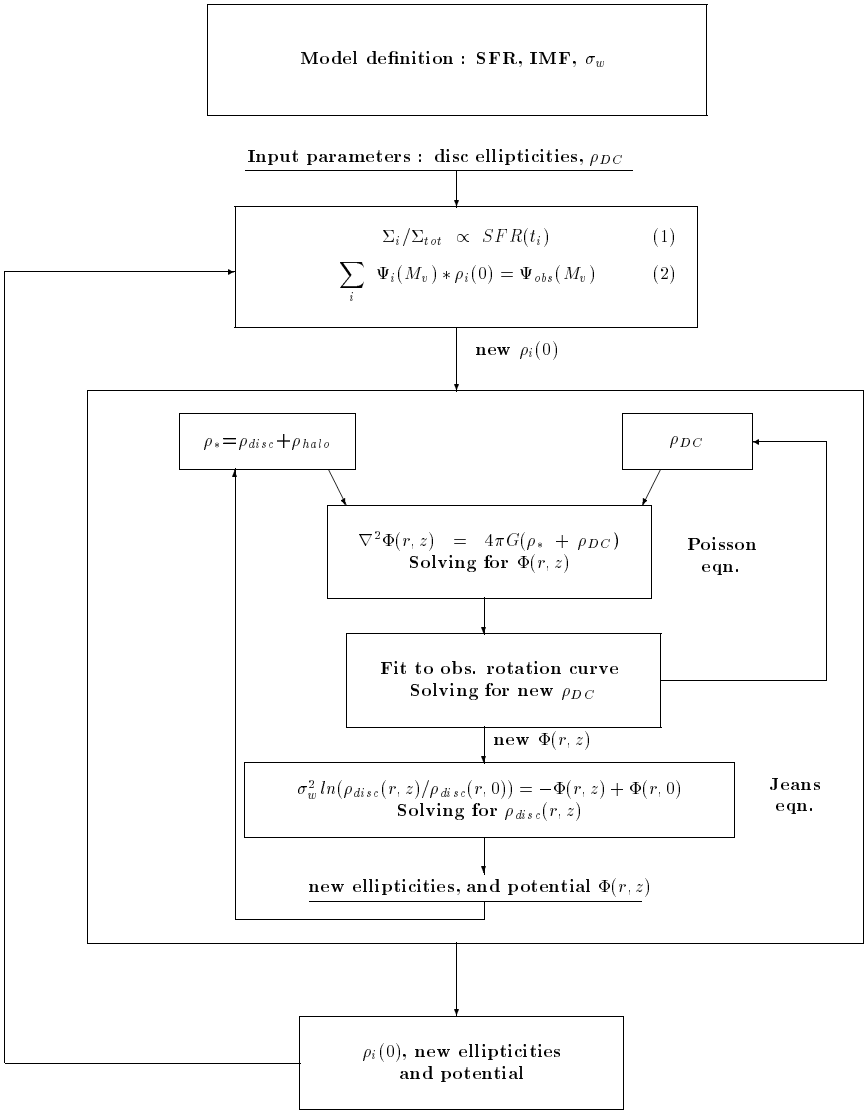

Fig. 1. Determination of a mass model for a given set of SFR, IMF, and age-σ_W relation using dynamical and observational constraints. Condition (1) establishes that at all times, the surface density of a given stellar disc age group stays proportional to the intensity of the star formation rate at the corresponding epoch (SFR(t_i)). Condition (2) forces the theoretical LF to have the same number of stars as the observed LF in the absolute magnitude range 5 to 10 and gives the model normalization. These two conditions permit to determine the $\rho_i(0)$. In the box below, a first guess of the potential is obtained by solving the Poisson equation and fitting the observed rotation curve, through the determination of dark corona parameters (ρ_{DC}). Below, the Jeans vertical equations is used to determine the new ellipticities for the stellar discs. With these new determinations, we return to conditions (1) and (2), etc. The process converges within a few loops.

since a 30% uncertainty in scale height confers an equivalent uncertainty in the local surface density of stellar material in the disc. More generally, one may question the accuracy of the exponential representation of the vertical density of disc stars. Given the fact that the disc heating is a time-dependent process, the number of stars found at a given height above the plane depends on how many stars were formed at a given epoch. In all studies the fundamental interplay between IMF, SFR and vertical structure has been neglected. The present paper focuses on the local constraints available for the discussion of these three aspects, while Paper II is dedicated to comparison with star counts at the galactic poles.

The paper is organized as follows. Sect. 2 summarizes the main features of the galactic disc model utilized. A set of models designed to represent the galactic disc stellar evolution is then proposed given different prescriptions for the SFR. In Sect. 3, we compute the density gradient in z for these models and compare them with the exponential profiles that are usually assumed for the galactic disc at solar radius. In Sect. 4, we discuss the accuracy of the IMF derived from the observed LF by various authors, then we study the LF by directly computing the LF with our model. We conclude in Sect. 5 and summarize the main questions that are to be addressed in Paper II.

2. Galactic disc model

The model of stellar population synthesis, from which the dynamical model utilized here originates, has been described at length in Robin & Crézé (1986), Bienaymé, Robin & Crézé (1987) (hereafter BRC) and Haywood (1994). A summary of the input parameters for the three stellar populations is given in Table 1 of Paper II. We give here a brief description of the model relevant to the disc population.

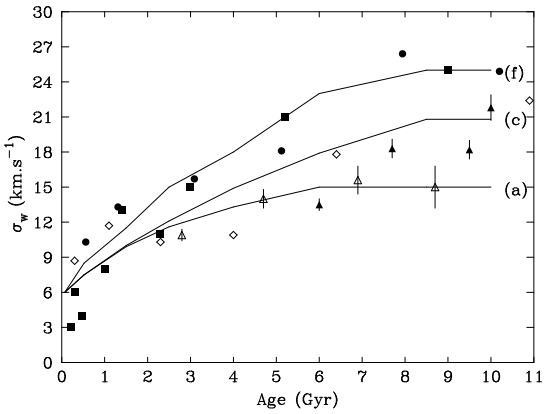

Fig. 2. The 3 age-σ_w relations tested in this study (continuous lines), and data from Mayor (1974) (circles), Wielen (1977) (squares), Strömgren (1987) (open and filled triangles), Meusinger et al. (1991) (diamonds).

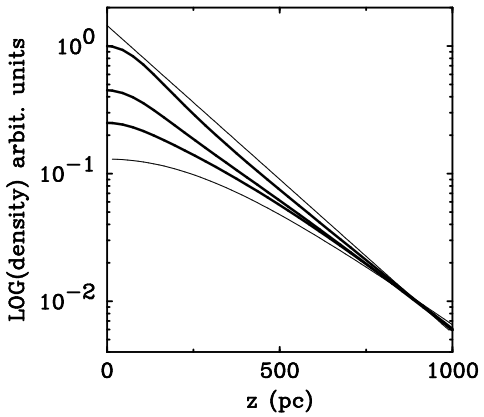

Fig. 3. Density profiles in the z direction for different SFR history in the galactic disc, normalized to have the same number of stars at large distance z. The thin continuous curves are exponential with a scale height 180 pc and sech^2 profiles. All other profiles have been calculated assuming age-σ_w relation $\mathscr{C}$, with exponential SFR of the form exp(-t/τ) and τ=-5, +∞, 5, from top to bottom.

2.1. General constraints

The characteristics of the disc stars are represented by the combination of two functions which describe their intrinsic properties and spatial distribution: $\Psi(M_v, Colour, Age) \times \rho(R, Z, Age)$. The Ψ function is the frequency distribution of the stars in the HR diagram, assuming a SFR history and IMF, which are the basic parameters that characterize a given disc model. A description of how the Ψ function is calculated is given in Haywood (1994), which also contains the detail of the various inputs (evolutionary tracks, bolometric corrections, B-V calibration etc...). The density distribution of the disc stars is given by the sum of 7 sub-populations, which analytic formula is given in BRC. It is considered that the 6 components older than 0.15 Gyr are isothermal, each component having its own velocity ellipsoid and age range. These are given in Sect. 3.1 (see also BRC).

The combination of the Ψ and ρ functions gives a consistent description of the galactic disc, provided that the age parameter in Ψ and in ρ refers to the same clock, linking dynamical and star formation histories. There are two observationally independent local constraints acting respectively on Ψ and ρ. The first one is the observed LF. The loose constraints on the evolution of the galactic disc provided by the local LF have been thoroughly reviewed by Scalo (1986) and are reconsidered here.

The second constraint is the observed age-σ_w relation, which is not used as a constraint in classical models. An intermediate stage on the way to dynamical self-consistency was reached by BRC, which permitted to use this relation. That is the velocity ellipsoids for the various populations are imposed in the model (instead of being deduced from the potential), but the vertical distribution of disc stars is calculated by integrating the Jeans vertical equation in the plane parallel approximation. The procedure, which leads to the local normalization and parameters for the vertical density laws of the disc, for a given SFR and IMF, is described in the flow-chart of Fig. 1. Using approximate values for the scale height of the disc, we calculate the volume density in the galactic plane for each subpopulation, by requiring that the relative value for each surface density complies with the prescription of the SFR (that is the relative importance of the surface densities in each age interval should correspond to the SFR intensities in these intervals). The second requirement is that the sum of the densities $\rho_i(0)$ matchs the value of the local stellar density. This is obtained by forcing the number of stars, calculated as a theoretical LF, to fit the observed LF, in the range of magnitudes where it is best determined, between M_v=5 and 10. This condition implies that the SFR in our simulation after 10 Gyrs (the age adopted for the galactic disc in our study), is not bound to satisfy the present SFR (as given by the LF at M_v<5). However, it is poorly determined and may not be representative of the SFR on the last Gyr, that is the time scale of interest here. Once this first estimate for the $\rho_i(0)$ is obtained, the calculation of the dynamical consistency described in Fig. 1 is applied.

The calculation that gives the scale height or disc ellipticities is described in detail in BRC. These parameters, which describe the scale heights of the disc density laws, are obtained for the values of the $\sigma_{w,i}$ and $\rho_i(0)$ for each subpopulation. Once these scale heights are obtained, new values of $\rho_i(0)$ must be calculated, to insure that they satisfy Eq. (1) and (2). Then new parameters for the scale height and new potential must also be calculated. The process converges within 2 to 3 loops.

For all the models presented below and in Paper II, the potential has been calculated assuming that there is *no* dynamically significant disc of dark matter in the solar neighbourhood. A surface density dark mass of 8 $M_\odot$.pc^{-3} has been assumed, and taken as an upper limit of the quantity of dark remnants in the solar neighbourhood. This is also within the error bars of the surface density found by Kuijken & Gilmore (1989).

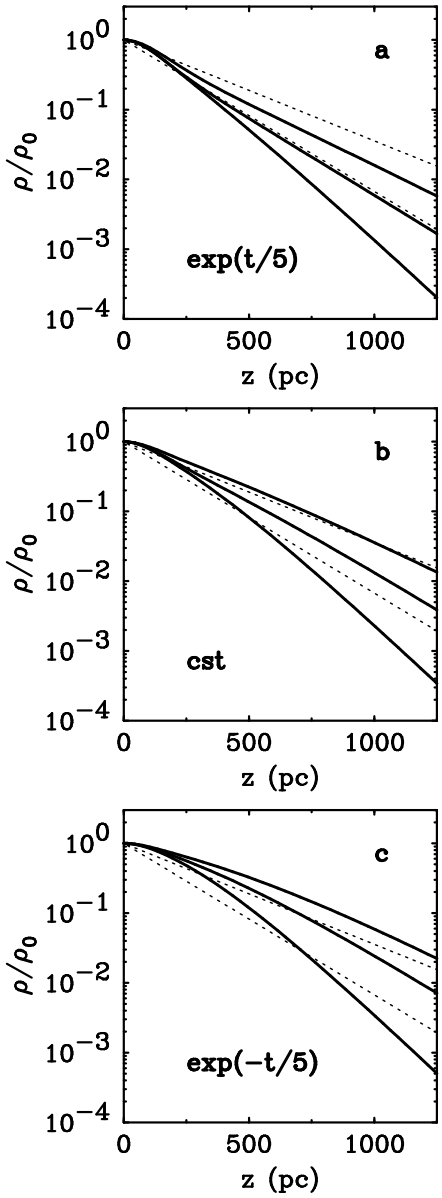

Fig. 4a–c. Density profiles obtained for different SFR and age-σ_w relations. From top to bottom, SFR are respectively increasing, constant and decreasing (defined as in Fig. 3). Each plot shows the profiles for the three age-σ_w relations $\mathscr{A}$, $\mathscr{C}$, $\mathscr{F}$ (respectively bottom, middle and top curves in each plot), and are normalized to 1 at z=0. Dotted lines are exponentials with scale height 200 and 300 pc.

2.2. SFR, IMF and age for galactic disc models

We have adopted the classical parametrization of the SFR as a simple exponential law exp(-t/τ), with τ=$\pm$ 5, $\pm$ 10, and ∞. The only concern here being the overall variation over the galactic disc lifetime, and not the details of the evolution. A value of τ=5 Gyrs represents a variation by a factor 7 of the star formation intensity throughout galactic disc history, for a disc age of 10 Gyrs. Justifications for adopting this upper limit are given in Sect. 4.

The IMF is represented by a power-law dN/dM $\propto$ M$^{-(1+x)}$, with 3 different slopes on 3 different mass intervals. The details of HR diagram computation are given in Haywood (1994). Let us just mention that we have used evolutionary tracks from Schaller et al. (1992) for stars with mass greater than 1 M$_\odot$, and from Vandenberg (private communication) for smaller masses. Evolutionary tracks for Helium-burning stars at masses between 1 and 1.7 M$_\odot$ are from Castellani et al. (1992). The age adopted for the galactic disc is 10 Gyrs.

3. The density profile in the z direction

At a given height above the plane, the disc in the model is therefore a sum of age-components, and the vertical density depends on both the age-σ_w relation and the SFR history. According to the observed age-σ_w relation, the oldest components must have the largest vertical extensions. This does not necessarily imply that old stars dominate counts: the relative importance of each component (i.e SFR history) plays a role too. The aim of the present section is to study what z-density profiles should be expected, considering the uncertainties in age-σ_w relation, which we briefly review in Sect. 3.1, and in SFR history in our Galaxy. Then, we discuss how these profiles compare with the exponential density laws used in most IMF investigations and galaxy models.

3.1. Observational measurements of the age-σ_w relation

The age-σ_w relation is known to vary very rapidly for the youngest stars: σ_w rises from approximately 6 $km.s^{-1}$ to 10-13 $km.s^{-1}$ within a few Gyrs (less than 3 Gyrs). Consequently, the young disc in the model cannot be considered isothermal and is divided in 4 different components of ages 0-0.15, 0.15-1.0, 1.0-2.0, and 2.0-3.0 Gyrs. The "old" disc is represented by 3 components of ages 3-5, 5-7 and 7 to 10 Gyrs. Unfortunately, no consensus has been reached on either the shape of the age-σ_w relation and the true level at which this relation saturates. In the model of the vertical distribution of stars, uncertainties in the age-σ_w relation produce effects which are of the same order of magnitude, or greater, as the effect generated by the SFR that we want to investigate, hence they must be taken into account. A review of the different empirical relations and the mechanism which are invoked to explain the increase of the velocity dispersion with age can be found in Lacey (1991). The present situation is summarized in Fig. 2, where we plotted four empirical age-σ_w relations from Wielen (1974), Mayor (1974), Meusinger et al. (1991), and Strömgren (1987).

Some authors suggested that Mayor and Wielen samples could be contaminated by thick disc stars (Strömgren (1987), Lacey (1991)). Strömgren (1987) divided his sample in two groups according to their metallicity, with a "pur disc sample" (-0.15< $[Fe/H]$ <+0.15) (empty triangles in Fig. 2) and a second group classified by decreasing metallicity (filled triangles). Oldest stars in the "pur disc sample" have σ_w which saturates at 15.3$\pm$2.8 km.s^{-1}, but goes to $\approx$ 21 km.s^{-1} for stars which may be classified as old disc stars according to their metallicity

Table 1. age-σ_w relations used in this work. Designations $\mathscr{A}$, $\mathscr{C}$ and $\mathscr{F}$ come from the larger set of relations given in Table 2 of Paper II.

	ages (Gyr)						
σ_w	**<.15**	**.15 - 1**	**1 - 2**	**2 - 3**	**3 - 5**	**5 - 7**	**> 7**
($\mathscr{A}$)	6.0	7.5	9.9	11.6	13.3	15.0	15.0
($\mathscr{C}$)	6.0	8.5	11.4	13.6	17.0	20.8	20.8
($\mathscr{F}$)	6.0	10.0	13.0	15.0	18.0	25.0	25.0

($[Fe/H] > -0.5$). The Meusinger et al. (1991) relation relies on a sub-sample of the Twarog (1980) data, representing 161 stars.

As can be seen from Fig. 2, data from Meusinger et al. (1991) are in satisfactory agreement with the sample from Strömgren (1987). A new sample of 189 F & G stars, with accurate age determinations, is given by Edvardsson et al. (1993). According to Freeman (1991), the age-σ_w relation shows a steep increase in the first three Gyrs, and then flattens at $\sigma_w \approx 20$ km.s^{-1}, also suggesting that Mayor & Wielen values could be overestimations.

In order to take into account the wide range of possible age-σ_w relations, either on the shape or the level at which these relations saturate, we have studied a set of 3 representative relations, displayed in Fig. 2 as thin lines and in Table 1. Relations ($\mathscr{A}$) and ($\mathscr{F}$) bracket the observed measurements of σ_w, while $\mathscr{C}$ is an intermediate relation.

3.2. Theoretical expectations

The dependency of the vertical density laws on the SFR history is qualitatively illustrated by Fig. 3, which shows the various profiles we obtained assuming the age-σ_w relation $\mathscr{C}$ and various exponential SFR. We note that the profile is very sensitive to the adopted SFR. As expected, the SFRs that must give greater weights to old stars get closer to a sech^2 law: decreasing SFR (lower thick curve) with τ=5 Gyrs gives rise to a density gradient which is not an exponential. With τ=5 Gyrs and an age for the disc of 10 Gyrs, the variation of SFR history is about 7. This is within the uncertainties of the star formation history (Sect. 4). On the contrary, the density profile obtained with the increasing SFR (upper thick curve) (exp(t/5)) is very close to an exponential, even when very near the galactic plane.

Fig. 4 shows how the density gradient changes with different SFR history and age-σ_w relations. Each plot shows the profile obtained for a given SFR, and for the three age-σ_w relations of Table 1. All these profiles are plausible according to present accuracies in the age-σ_w relation and SFR history. The difference in the densities at a given distance due to uncertainties in the age-σ_w are very large. In the case of the constant SFR (Fig. 4b), this difference amounts to more than 65% at z=500 pc, between profile $\mathscr{C}$ and $\mathscr{F}$ and 170% between profile $\mathscr{A}$ and $\mathscr{F}$ at the same distance.

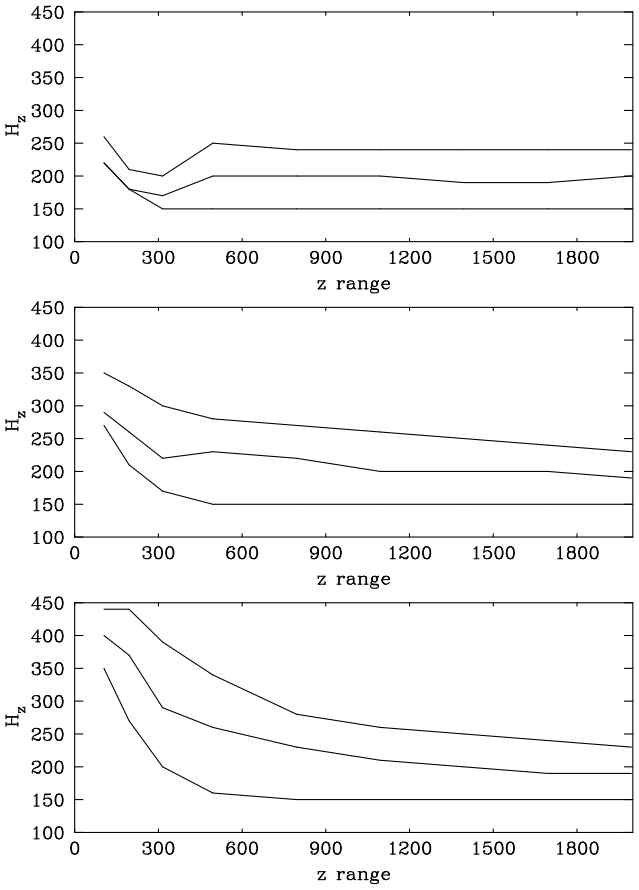

Fig. 5a–c. Scale height (y-axis) of the exponential function best fitting each of the density laws of Fig. 4, between galactic plane and z=2000 pc. Plot **a** is for increasing, **b** constant and **c** decreasing SFR. The value of the best scale height can be read on the y-axis.

3.3. Questioning the exponential approximation

The exponential scale height is an unneccessary restrictive concept in the case of the BRC model, however, it is instructive to investigate how exponentials compare with a more sophisticated model, as most pictures of the large scale structure of the Galaxy are based on this assumption. The comparison with our models will show that this approximation is too crude. Paper II will demonstrate that it is probably responsible for misleading interpretation of star count data.

3.3.1. Brief review

In 1980, Bahcall & Soneira presented a model of the Galaxy with the galactic disc density law based on the exponential approximation, justified by a long lasting accepted convention but rather weak observational facts. In the eighties, mainly two results have provided more solid support for the exponentials as convenient fitting functions, concomitantly with the renewal of galactic models. The first one is the work by Gilmore and Reid (1983), where it was shown that the observed vertical density distribution is well represented by two exponentials at z<4000 pc.

This fact is reconsidered in Sect. 6.1.2 of Paper II. The second one is the numerical calculation by Bahcall (1984) of the disc density law that comes out from his dynamical model. Bahcall demonstrates that the numerical integration of the Poisson-Boltzmann equations for the parameters of the disc given in Bahcall & Soneira (1980) gives a vertical density distribution at 300<z<900 pc very near to what one would obtain using an exponential. This result is confirmed by our own calculation. Examining the Table 4 of Bahcall (1984), the relative weights attributed to his different kinematic components (with σ_w=4, 10, 13, 15, 20, 24 km.s^{-1}) are very similar to those we find in our model for a constant SFR (for *this* model, Fig. 4 shows that between 300 and 900 pc, the exponential is a satisfactory approximation). However, there is a significant contradiction between this result of Bahcall (1984) and the star-count model of Bahcall & Soneira (1980) : the disc scale height deduced from his dynamical analysis is around 200 pc, whereas the scale height used in the (star-count) model is 325 pc. We note that this contradiction has not been addressed in subsequent dynamical or star-count analysis. After Bahcall & Soneira (1980), most models have used the value of 325 pc, and have found satisfactory agreement with star count data. It is only recently that an obvious discrepancy has been found between this standard model and observed star-counts (Reid & Majewski, 1993), but without seriously questioning the exponential approximation. In passing, we note that the red dwarfs detected by Majewski (1992) are at typical distances of 1000-2500 pc, whereas Bahcall (1984) specifies that the agreement between exponential and his dynamical model is found to be statisfactory only in the distance range 300 to 900 pc. Outside these limits, the discrepancies are of less than 25% between 900 and 1000 pc and at z<300 pc, but unspecified for distances beyond 1000 pc. With the availability of more accurate and extreme data, such as Majewski's (1992), this approximation needs to be reconsidered.

3.3.2. Comparison with our model

The inadequacy of exponentials to represent the more realistic profiles of Fig. 4 is shown in Fig. 5. Each curve in Fig. 5 gives the exponential scale height (y-axis) that should best-fit the profiles of Fig. 4, at various distances above the plane (x-axis). Each scale height was obtained by calculating χ^2 fits between exponentials and our profiles over 300 pc distance ranges, without forcing the density profiles to have the same normalization. Obviously from Fig. 5, a single exponential is not adequate to describe the density variation at z< 500 pc, whatever the SFR history or age-σ_w relation. The most dramatic difference is for the decreasing SFR. For example, with the age-σ_w relation $\mathscr{C}$, the exponential scale height varies from 300 and 230 pc between z=100 and 500 pc. It should be noted also that there are very few profiles which, at distances greater than z=300 pc, can be fitted with a scale height of 300 pc or higher. This is the case only for profiles corresponding to age-σ_w relation $\mathscr{F}$ and constant or decreasing SFR. For a constant SFR, and age-σ_w relation $\mathscr{F}$, which is the model which presents the closest characteristics with Bahcall (1984), the scale height at z<1000 pc is

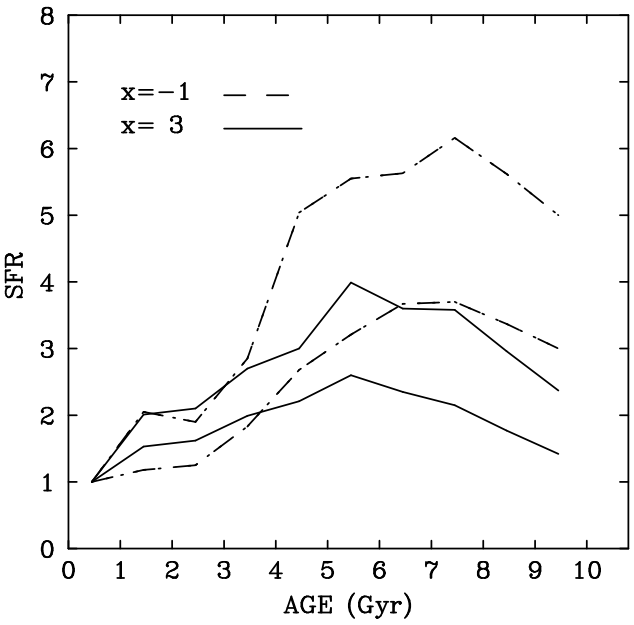

Fig. 6. The SFRs from Twarog (1980) for x=-1 (dashed-dotted curves) using scale height corrections from age-σ_w relation ($\mathscr{A}$) (lower curve) and ($\mathscr{F}$) (upper curve). Continuous curves are for x=3, and same age-σ_w relations.

greater than 250 pc, whereas Bahcall found 203 pc. The main difference responsible for this discrepancy is, of course, the huge amount of dark matter in Bahcall's model, equal, in volume density, to the visible matter. The increasing SFR provides profiles which are much closer to exponentials at z>500 pc. This is true also for the two other SFR and age-σ_w relation $\mathscr{A}$. However, the scale height here is of about 150 pc, very much lower than the observed 250-350 pc.

Now, does the use of exponential profiles explains why star-count models adopted scale height of 325 pc, while our model has smaller disc thickness ? Anticipating our discussion on star-count fitting with Galaxy models of Paper II, we want to make the following comment. Let us suppose that star-count data at the galactic pole are adequately described using the profile $\mathscr{C}$ on Fig. 4b (constant SFR). Had we used instead an exponential law with scale height 300 pc, normalized to the local LF (as shown in Fig. 4), the net effect would be that we would approximately match the number of disc stars at z<400-500 pc, (the χ^2 shows that the best fit to profile $\mathscr{C}$ (constant SFR) for z<300 pc is found for h$_z$ ≈300 pc), while the exponential is an overestimation beyond z>400-500 pc. Looking at galactic pole predictions of our star-count model (Paper II), most disc stars brighter than V=14 lay below 400 pc while most stars fainter than V=15 lay beyond 400 pc, but not all of them are disc stars, since thick disc rapidly increases. Consequently, using an exponential law with h$_z$=300-350 pc, disc stars may be (roughly) correctly estimated at V<15 and z<500, while they could be severely overestimated at V>15. This is of great consequence for star counts at faint magnitudes, in particular because, if disc stars are overestimated, we expect that thick disc stars at the same magnitudes

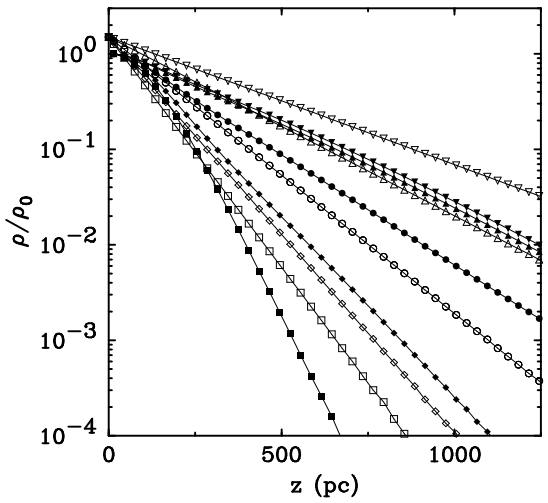

Fig. 7. Comparison of the exponential profiles used by Scalo (1986) (empty symbols) and the one deduced from our model (filled symbols), normalized to 1 at z=0, and for different absolute magnitudes. The thickening of the disc in our model is described through age-σ_w relation $\mathscr{C}$, and the age distribution of stars along the main sequence was calculated assuming a constant SFR. Squares are for M_v=0, diamonds for M_v=2, circles M_v=3, triangles for M_v=4 and 5.

will be *underestimated*. This point is discussed in further detail in Paper II. Eventually, KTG (1993) found their data to be compatible with a constant number density at z<80 pc. Such a feature is clearly present in our simulation (see profile $\mathscr{C}$ in Fig. 4b).

4. Solar neighbourhood SFR and IMF

In the following, we briefly discuss the uncertainties that affect the SFR history, as obtained from the study of solar neighbourhood stars. Then, we assess the accuracy of the IMF derived from the solar neighbourhood LF.

4.1. Uncertainties in the SFR

The history of the stellar birthrate in the solar neighbourhood has been derived through several techniques over the last 20 years. A general feeling from many different studies is that the birthrate in the galactic disc remained more or less constant since the formation of the disc. However, it is difficult to assess what "constant" means exactly because quite different assumptions have been made regarding the disc dynamical evolution and the adopted scale heights.

For instance, the SFR found by Twarog (1980) (irrespective of uncertainties due to stellar evolution theory and main sequence datation) hinges on the IMF slope in the mass range of 1 to 3 solar masses, and scale height corrections. The IMF in this mass range is usually assumed Salpeter-like (x=1.35) or Scalo like (x=1.7) for which Twarog's SFR has a maximum equal to about three, 9 Gyrs ago, with a subsequent slow decrease. However, there is *no* evidence that the IMF slope in the mass range 1-3 $M_\odot$ is around x=1.3-1.7. Quoting Twarog (1980) study for a constant SFR, often used in galactic disc models, would implies a corresponding very steep IMF in the intermediate mass range, in the order of x=3. The decreasing SFR envisaged by Twarog (1980), corresponded to a flat slope for the IMF (x=-1), according to his data. Scalo (1986) has favored a bimodal IMF on the basis of his LF study, also implying a decreasing SFR.

As an illustration of the SFR uncertainties originating in the age-σ_w relation, we have calculated the scale height of a given isothermal population of stars embedded in a disc made of several components using the formula of Talbot & Arnett (1975):

$$h_{z,i} = \sigma_{w,i}/(2\ \pi\ G\ \sum_i\ \rho_i(0))^{0.5} \quad (1)$$

The relevant quantity here is the ratio h_i/h_0, which we have calculated in the case of the relation ($\mathscr{A}$) and ($\mathscr{F}$). Applying these scale height ratios to the data of Twarog (his Table 3, column 4, 6), the SFR variations we obtain are displayed in Fig. 6, for IMF x=-1 and x=3. As can be seen from the figure, the SFR still covers a wide range of possible variations, from decreasing SFR by a factor of 6, to first increasing and then decreasing SFR, by a factor of 2.5. In 1977, Mayor & Martinet had reached a similar conclusion, and were not able to constraint SFR variation to better than a factor of 7.

Other methods have made use of the white dwarf LF and the chromospheric activity of red dwarfs, the uncertainties and advantage of each being well described in the recent papers of Wood (1992), Yuan (1993) and Soderblom et al. (1991). The accuracy on the SFR determination using the white dwarf LF is also limited to within a factor of 7.

4.2. Uncertainties in the IMF

A widely used method to estimate changes between past and present SFR is the study of the shape of the LF. A comprehensive review on this issue was given by Scalo (1986). The LF gives a measure of the variation between the mean SFR in the galactic disc since its formation and the present-day SFR. The fast change of star lifetimes along the main sequence implies that most stars seen at M_v<1 are young, and therefore witness the SFR at the present epoch whereas stars at M_v>4 are long-lived stars (t_{ms} greater than the age of the galactic disc), and their number gives the mean intensity of the SFR since the beginning of star formation in the disc. As emphasized by Scalo (1986), the ratio $SFR(now)/ < SFR >$ gives a hint to the overall variation of the SFR provided the present SFR is not special in any respect. For instance, if star formation in the Galaxy proceeds as a succession of burst, as has been suggested (Scalo, 1988), then this ratio is barely a meaningful measurement of the overall SFR variation.

In the restricted range of magnitude 1 $\leq M_v \leq$ 4, the LF depends on both the IMF and SFR history. Scalo (1986) has investigated the possible shape of the IMF assuming different SFR histories. He favoured a bimodal IMF (see his Fig. 17) assuming two modes of star formation, dominant at masses m=0.3

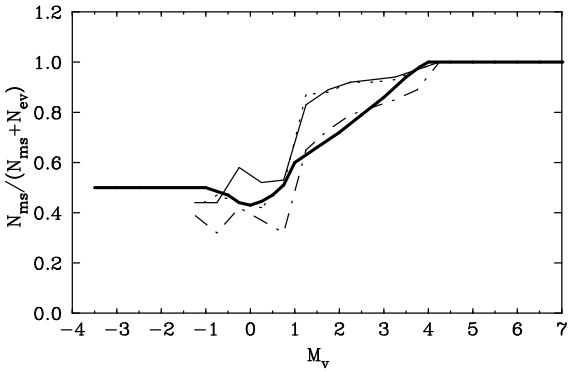

Fig. 8. The ratio of main sequence stars to (main sequence + evolved) stars as a function of M_v. Three models are shown on the figure, dotted curve is for increasing SFR, continuous thin curve is for constant SFR, while dashed-dotted is for decreasing SFR. The thick line is the relation adopted by Scalo.

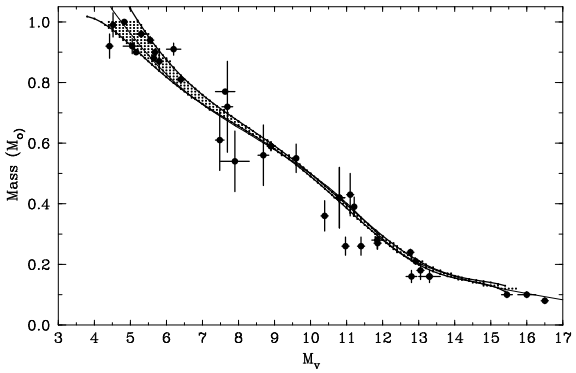

Fig. 9. The Mass-M_v relation as deduced from our model (dotted area) and the two continuous thick lines which are polynomial fits limitting this relation. The thin continuous line is the mean relation adopted by KTG (1993). Most observational points are from Popper (1980).

and m=1.1-1.3 $M_\odot$. We discuss below the different conversion factors that are required to obtain the IMF from the LF, and the accuracy of the new IMF we obtain. A second method, utilized in Sect. 4.3, consist of calculating theoretical luminosity functions, as described in Haywood (1994), and compare them with the observed one. An interesting consistency check which we also discuss in Sect. 4.3 is to use the (IMF,SFR) derived with the first method as input parameters to the second.

Information about the present-day mass function (PDMF) is usually obtained by applying the following transformations to the LF (Miller & Scalo, 1979):

$$\Phi(m) = \frac{dM_v}{dm} * 2 * H(M_v) * f_{ms}(M_v) * \Psi(M_v) \qquad (2)$$

which include the derivative of the absolute magnitude to mass relation, the correction for the increase of the scale heights of the stars with absolute magnitude, H(M_v), and the corrections for the percentage of evolved stars at a given absolute magnitude, f_{ms}(M_v).

These last two factors depend on the history of the galactic disc. For instance, the ratio of the evolved to main sequence stars ought to be high if the SFR was greater at remote times. Similarly, it is expected that main sequence stars at a given magnitude are a mixture of ages with different characteristics scale heights, oldest stars having the largest scale heights. The final scale height at a given magnitude will therefore depend on the relative weight of each of these age groups, and hence on the star formation history. These may be second order effects compared to the other uncertainties (particularly the uncertainty in the mass-absolute magnitude relation), but it is nonetheless necessary to quantify them.

4.2.1. Scale heights correction

For the conversion from volume density to surface density, the method described in Sect. 4.2 uses a mean absolute visual magnitude-scale height correction. We may calculate, using our model, the h_z-M_v relation one would obtain, adopting for example a constant SFR and the age-σ_w relation $\mathscr{C}$. This relation is illustrated in Fig. 7, where we have plotted the exponential density laws as given by Scalo (1986), and the density profiles we obtained with our model. Only the integral under each curve is important, not the detailed density variation. We may calculate an equivalent exponential scale height to our model curves, by dividing the surface density with the volume density. The scale height corresponding to unevolved dwarfs (triangles) is approximately 260 pc if the age-σ_w relation $\mathscr{C}$ is the correct relation. The scale height one would obtain with age-σ_w relation $\mathscr{F}$ would be $\approx$ 345pc, more akin to the one adopted by Scalo (1986). In the case for decreasing SFR, and with this last age-σ_w relation, the equivalent scale height would be $\approx$ 380pc. Fig. 7 also shows that the relation of Scalo systematically underestimate the scale heights of stars with M_v=2 and 3, therefore underestimating their surface density.

4.2.2. Correction for evolved stars

To illustrate how this factor depends on the star formation history in the disc, we have plotted in Fig. 8 the correction for evolved stars that one has to apply to the LF, as it comes out of our model (i.e assuming the evolutionary tracks mentioned in Sect. 2.2), and for different SFRs. The thick curve is the one adopted by Scalo (1986). The continuous and dotted curves correspond to constant and increasing SFR respectively. They differ significantly from the curve adopted by Scalo, which decreases to 0.6 at M_v=1 while our model indicates more than 0.8 if the SFR has been constant or decreasing. In this region, the stars belong mainly to the main sequence and to the subgiant branch. Main sequence lifetimes vary from 10 Gyrs to 1 Gyrs according to evolutionary tracks, while subgiant branch time scale is approximately 10 time smaller.

The curve given for a decreasing SFR (factor 7) bears some ressemblance with the one adopted by Scalo. The decrease in

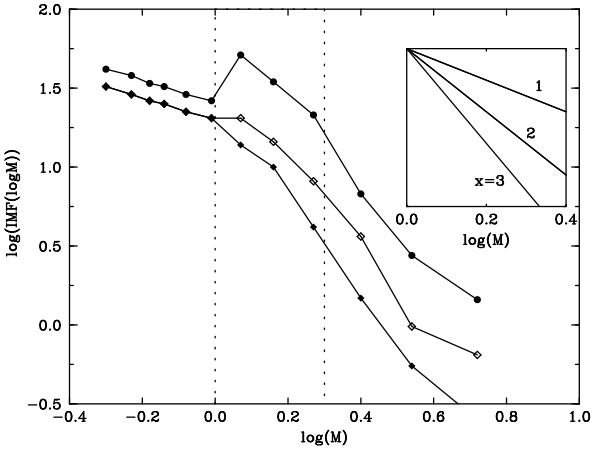

Fig. 10. The IMF in the solar neighbourhood derived using the new factors in Table 2. The upper IMF corresponds to the decreasing SFR, calculated with scale height corrections from Scalo. The two others curves are for constant and increasing IMF (lower curve), calculated assuming a scale height of 250 pc at M_v >4, and Scalo corrections otherwise. Dotted vertical lines give the limit for 1 and 2 solar masses, while the indexes indicated in the box are for power-law IMFs with $dN/dM \propto M^{-(1+x)}$.

main sequence/evolved stars in the range M_v=1-4 is similar to Scalo's, while it seems to shows less evolved stars.

4.2.3. The mass-M_v relation

Scalo (1986) quoted in his review that mass-M_v is probably the most important source of uncertainty in the derivation of the IMF. We want to point out here its importance for the IMF at masses less than solar. Scalo advocated that the IMF is bimodal, because the shape of the observed LF at M_v=5-9, shows a flattening or a dip that he attributed to an equivalent feature in the mass function. He demonstrated that this dip was followed by a rise in the IMF with a maximum at 1.3 $M_\odot$, if a constant or decreasing SFR was assumed. Scalo favoured the case of a decreasing SFR and an age for the disc of 15 Gyrs, therefore implying strong bimodality. At the same time, D'Antona & Mazzitelli (1986) showed that the mass-M_v relation could be responsible for the flattening in the LF if the non-linear variation of the luminosity with mass was taken into account, a result further demonstrated by KTG (1990, 1991, 1993) and Haywood (1994).

Although these studies have weakened the argument for a dip in the mass function at 0.5-1.0 $M_\odot$, there remain surprising differences between the value derived by D'Antonna & Mazzitelli and Haywood (1994) ($x \approx 0.7$) on the one side, and KTG(1993) (x=1.2) on the other side. Such a difference is not expected, because the LF is known to have satisfactory accuracy in the magnitude range M_v=5-10. Because the LF used in all three studies is the same, the only difference is the mass-M_v relation. In DM and KTG, the link between the mass and the magnitude is a one-to-one relation, while in Haywood (1994), the LF was computed through the evolution of stars on tracks over a period of 10 Gyr. The resulting area spanned by the stars over the mass-M_v plane is shown in Fig. 9. The thin continuous curve on the figure is the relation adopted by KTG, which, as can be seen agrees well with our own relation. However, adopting a mean mass-M_v relation becomes a rough approximation when its derivative has to be taken for the conversion to mass. As an illustrative example and in order to explain the difference between our result and the one of KTG, we have considered two other mass-M_v relations, which are shown in Fig. 9 as thick lines, and are polynomial fits that bracket the mass-M_v relation obtained from evolutionary tracks. We then simply calculate their derivatives, and the corresponding IMF.

If we use the derivative given by KTG (their figure 2), we found an IMF which is adequately fitted by a straight line. A minimum χ^2 fit shows that its slope is x=1.15, a value that is (not surprisingly) in agreement with the one given by KTG(1993). However, the slopes obtained with our two polynomial fits are 1.15 and 0.43, which is the range of uncertainty that results from this method. Hence we cannot decide what is the best slope for the IMF within this range; the two slopes derived here are equally representative of the local IMF derived by this method, but none of them tell us what is the true IMF. A correct measurement of the IMF at M>0.5 $M_\odot$ must take into account the distribution in magnitude at a given mass. This can only be done by taking into account the luminosity evolution of the stars over their main sequence life. In Haywood (1994), such a calculation was done, and we found that the IMF was correctly represented using an index of 0.7 at M<1 $M_\odot$, which is a more exact value of the IMF slope. It is the value adopted hereafter.

4.2.4. The solar neighbourhood IMF revisited

Evaluating the uncertainty in the IMF due to assuming the derivative of a mean mass-M_v relation at masses higher than solar becomes a difficult and unproductive task. Although the computation of theoretical LF depends on stellar evolution theory, it does not rely on fragile approximations (mean mass-M_v relation, hypothetical evolved to main sequence ratio etc..). It is a much more straighforward procedure, and one that offers the advantage of comparisons that can also be made on the evolved stars contained in the LF. This will be done in the next section. We want to illustrate now what are the possible IMF when taking into account all the uncertainties discussed above.

Having eliminated the possibility for a dip in the IMF at M=0.7-0.8 $M_\odot$, we return to a problem mentioned by Miller & Scalo (1979): if one assumes a constant or decreasing SFR, the corrections for evolved stars are important, and give rise to a change of behaviour in the IMF at M=1 $M_\odot$, which could be assigned to bimodality. As noted by Miller & Scalo (1979), it is quite problematic that the rise in the IMF appears just at 1 $M_\odot$, which designates the mass of our sun as being special. We now derive new IMFs, assuming an age for the galactic disc of 10 Gyrs (therefore minimizing the correction for SFR history), to see how this feature is present in our calculations. These IMFs are plotted in Fig. 10 and given in Table 2. The IMF at M<1 $M_\odot$ is the one obtained for x=0.7. At M>1 $M_\odot$ we adopt the mass-M_v relation of Scalo (1986).

Table 2. IMF given different assumptions on the SFR and scale height of the disc. Columns (1) to (5) give the absolute visual magnitude, the mass, the observed luminosity function, the derivative of the mass-M_v relation, the scale height corrections. Column (6) gives the IMF assuming a constant SFR and for scale heights corrections of column (5). Column (7) gives the IMF obtained with an exponentially increasing SFR with a characteristic time scale of 5 Gyrs, and with the same scale height corrections. Column (8) gives the scale height corrections of Scalo (1986), and column (9) the IMF when an exponentially decreasing SFR with a characteristic time scale of 5 Gyrs and scale height corrections of column (8) are assumed. The IMF at M<1 $M_\odot$ is calculated assuming x=0.7, starting from m=0.962 $M_\odot$.

M_v (1)	m (2)	log$\Phi(M_v)$(3)	$\frac{dM_v}{dlogm}$ (4)	2H (5)	Cst (6)	Inc (7)	2H (8)	Dec (9)
10	.	-2.13	.	500	1.51	1.51	650	1.62
9	.	-2.33	.	500	1.46	1.46	650	1.58
8	.	-2.41	.	500	1.42	1.42	650	1.53
7	.	-2.52	.	500	1.40	1.40	650	1.51
6	.	-2.44	.	500	1.35	1.35	650	1.46
5	0.962	-2.49	12.8	500	1.31	1.31	650	1.42
4	1.139	-2.62	10.6	400	1.31	1.14	500	1.71
3	1.445	-2.80	9.20	340	1.16	1.00	340	1.54
2	1.862	-3.16	8.10	230	0.91	0.62	230	1.33
1	2.512	-3.60	7.10	160	0.56	0.17	160	0.83
0	3.467	-4.18	6.40	140	-0.01	-0.26	140	0.44

Fig. 10 illustrates the very great uncertainties that remain in the IMF, due mostly to scale height corrections, and to our ignorance of the SFR history. Because of scale height corrections, the IMF at masses less than solar remains uncertain up to at least 20 to 30 %. At masses greater than solar mass, the conjugated effects of the scale heights and SFR, the number of stars that formed within this mass range is uncertain to a factor of 5-10. In the case of the constant and increasing SFR, the IMF in Fig. 10 is compatible with a smooth IMF, and we think that although the IMF shows a flattening at 1.0-1.1, no bimodality is apparent, given the uncertainties that still remain, in particular due to the adopt of a mean mass-M_v relation. At masses greater than 1.1 $M_\odot$, the IMF corrected for a constant SFR may be represented with a slope x ≈2.0-2.2, depending on the considered upper mass (log M=0.27 or 0.4). In the case of the increasing SFR, the IMF is near x=2.6-2.9 over the same mass range.

On the contrary, if a decreasing SFR is assumed, the change in the IMF at 1 $M_\odot$ leans in favour of a bimodal IMF, and the problem raised by Miller & Scalo is relevant. As mentioned above, either we should considered that the mean mass-M_v relation is responsible for the problem, or that the history of the SFR is not one which has decreased over the last 10 Gyrs.

4.3. Synthetic luminosity function

One way to check how the results found by Scalo (1986) or hereabove are consistent with the observed LF is to use the IMF derived through the present-day mass function and the corresponding SFR as input parameters to compute theoretical LF using synthetic HR diagrams. Fig. 11 presents a number of theoretical LF that are compared with the observed LF. Two observed LFs are shown: the LF from Scalo (1986), which was used to obtain the IMF in the last section, and the LF from Wielen et al. (1983). The characteristics of the model used for each curve are given in Table 3.

Table 3. Characteristics of each model used to calculate the LFs of Fig. 11. The first column gives the number of the curve on each of the plot of Fig. 11. The 3 power law IMF slopes are given over the mass ranges M<1.0 $M_\odot$, 1-3 $M_\odot$, and M>3.0 $M_\odot$. T_0 is the disc age.

	SFR	T_0 (Gyr)	IMF	acceptable ?
1	exp(-t/12)	12	Scalo (1986)	no
2	exp(-t/10)	10	Scalo corrected	no
3	exp(-t/10)	10	0.5/1.5/2.0	yes
1	cst	12	0.7/0.0/2.0	no
2	cst	10	0.7/1.5/2.0	yes
3	cst	-	0.7/2.0/2.0	yes
4	cst	-	0.7/2.5/2.0	yes
1	exp(t/5)	10	0.7/1.5/2.0	no
2	exp(t/5)	-	0.7/2.5/2.0	yes
3	exp(t/5)	-	0.7/3.5/2.0	yes

In Fig. 11a, the curve labelled 1 is the LF obtained for an exponentially decreasing SFR exp(-t/τ) (τ=12 Gyrs) and an age for the disc of 12 Gyrs, while the other two curves were obtained for an age of 10 Gyrs. The IMF is the one given by Scalo (1986) for the same parameters (see his figure 17). The curve labelled 2 was obtained for the IMF of Sect. 4.2.4 that corresponds to a decreasing SFR (see Fig. 10). Finally, the curve labelled 3 is for an IMF with a slope 0.7/1.5/2 on mass intervals 0.1-1.0, 1.0-3.0 and >3 $M_\odot$, and the same SFR.

It is striking to see how the LF (1) in Fig. 11a, calculated with the IMF given by Scalo (see his Fig. 17), contradicts the result obtained by Scalo. Clearly such a combination of IMF and SFR does not yield an acceptable fit with the observed LF. This calculated LF tells us that if a decreasing SFR is the true SFR, then necessarily something was wrong in the derivation of the IMF by Scalo (1986), most probably his mean mass-M_v relation. This point of view is confirmed by the curve (3) in Fig. 11a: since the fit to the observed LF is correct in this

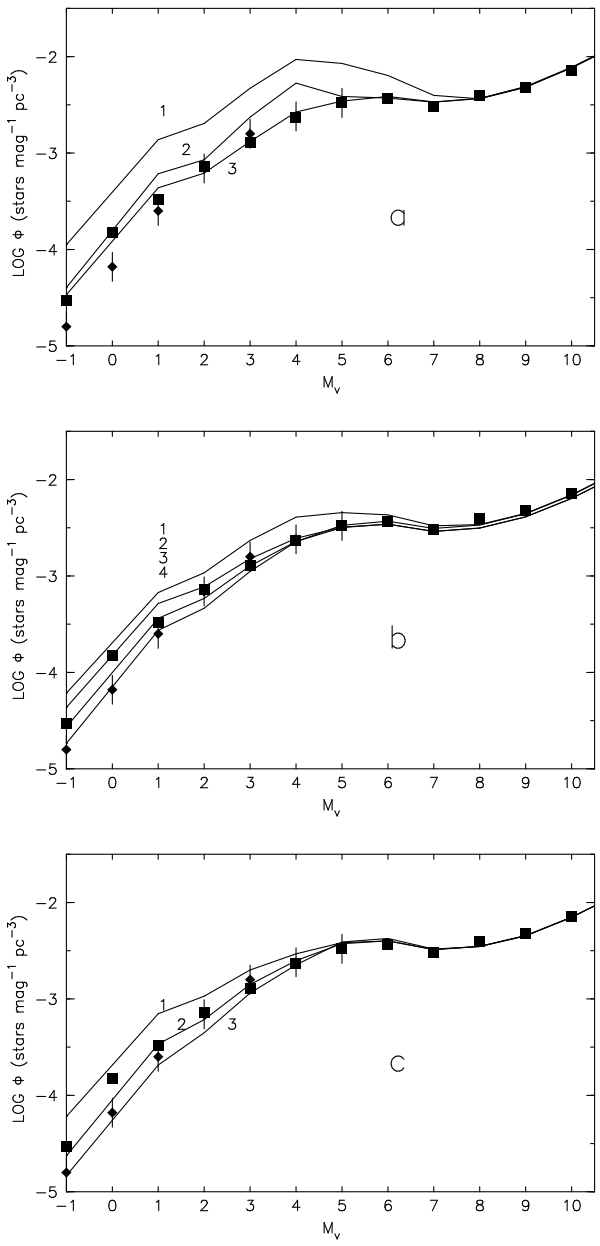

Fig. 11a–c. LFs obtained for different SFRs and IMFs. The observed LF in Scalo (1986) (dots, M_v<4), and Wielen et al. (1983) (squares). Plot **a** is for decreasing SFR, **b** is for constant SFR, and **c** increasing SFR. See text for detail.

case, according to our synthetic LF, a decreasing SFR implies an IMF with a slope of x=1.5, in contradiction with the strongly bimodal IMF found by Scalo. The same effect is present in the case of LF (2), while the difference with the observed LF is much smaller, due to the fact that we considered the change of slope in the IMF at 1.0 $M_\odot$ (and not at 0.7 $M_\odot$). The bump at M_v=4 corresponds to the maximum at M=1.17 $M_\odot$ in the mass function (see Fig. 10).

In Fig. 11b, LF (1) was obtained for a disc age of 12 Gyrs, with IMF slopes 0.7/0.0/2, chosen to represent the similar IMF Scalo derived assuming a constant SFR (see his Fig. 17). Here again, his IMF overestimates the number of stars in the range 0.7 to 1.17, and the LF appears systematically higher than the observed one. In view of the uncertainties in the data, the LF (2, 3, 4) all look acceptable IMF.

In Fig. 11c, the increasing SFR with a IMF slope x=1.5 yields an LF which systematically overestimates the observed LF at M_v>3. IMF with x=2.5 falls well within the range of observed LFs. IMF slope x=3.5 gives the upper limit of acceptable IMFs.

5. Conclusions

The vertical structure of the galactic disc results from the combined effect of the star formation history and the secular heating of the disc. Combining these two factors in a dynamical consistent model, within the range of possibilities left open by local contraints, we get the following conclusions.

The shape of the vertical density law strongly deviates from the classical exponential even though this approximation may hold over restricted distance ranges. At low distances (say below 500 pc), a single exponential is inadequate under any reasonable scenario.

Concerning the IMF, the synthetic approach used here where the predicted solar neighbourhood luminosity function comes out strait from the combination of SFR, IMF, via reliable evolutionary tracks strongly reduces the dependence of the result on arbitrary mass-M_v relations. As a result the bimodal IMF derived by Scalo (1986) in association with a decreasing SFR turns out to be most likely an artefact due to the crude mass-M_v approximation.

Within the possibilities left open by realistic vertical density profiles, and by compatibility with the observed luminosity function, the range of possible star formation scenarii (IMF+SFR) is significantly reduced yet not pointing to a unique solution. These include a decreasing SFR with an IMF index $\leq$1.5, a constant SFR in combination with an IMF index of $\approx$2, or an increasing SFR with an IMF index $\geq$2.5. The age-σ_w relation (i.e typical timescale of dynamical heating) is also an important residual source of uncertainty. In Paper II we shall show that faint star counts at the galactic poles can help removing these ambiguities.

Acknowledgements. It is a pleasure to thank I.N. Reid for several interesting and stimulating discussions and suggestions, which much improved these two papers. This work is a part of MH's PhD thesis and was partially supported by the Indo-French Center for Advanced Research/Centre Franco-Indien pour la Promotion de la Recherche Avancée.

References

Bahcall, J., & Soneira, R.M., 1980, ApJS 44, 73
Bahcall, J., & Soneira, R.M., 1981, ApJ 246, 122
Bahcall, J. 1984, ApJ 287, 926
Bienaymé O., Robin A. C. & Crézé M., 1987, A&A 180, 94
Castellani V., Chieffi A., Straniero O. 1992, ApJS, 78, 517
D'Antona, F. & Mazzitelli, I., 1986, A&A, 162, 80

Dahn C. C., Liebert J., Harrington R. S., 1986 AJ, 91, 621
Edvardsson B., Andersen J., Gustafsson B., Lambert D. L., Nissen P. E., Tomkin J., 1993, A&A 275, 101
Freeman, K, 1991, Dynamics of Discs Galaxies, Ed. B. Sundelius
Gilmore G.F., 1984, MNRAS 207, 223
Gilmore G.F. & Reid I.N., 1983, MNRAS 202, 1025
Haywood, M., 1994, A&A 282, 444
Kroupa P., Tout C., Gilmore G.F. 1990, MNRAS, 244, 76
Kroupa P., Tout C., Gilmore G.F. 1991, MNRAS, 251, 293
Kroupa P., Tout C., Gilmore G.F. 1993, MNRAS, 262, 545
Kuijken K. & Gilmore G., 1989, MNRAS 239, (571,605,651)
Lacey C. , 1991, Dynamics of Discs Galaxies, Ed. B. Sundelius
Larson R.B. 1986, MNRAS, 218, 409
Majewski S.R. 1992, ApJS 78, 87
Mayor M., 1974, A&A 32, 321
Mayor M. & Martinet L., 1977, A&A 55, 221
Meusinger H., Reimann H.-G., Stecklum B.,1991, A&A 245, 57
Miller G.E. & Scalo J. M., 1979, ApJSS 41, 513
Ojha D.K, PhD Thesis, Obs. de Strasbourg
Popper D.M. 1980, ARA&A, 18, 115
Reid N. & Majewski, 1993, ApJ 409, 635
Robin A.C., Crézé M. 1986, A&A, 157, 71
Scalo J. M, 1986, Fund. Cosm. Physics, 11, 1
Scalo J. M, 1988, XXIInd Moriond Astrop. Meeting, Starbursts & Galaxy Evolution, Eds. Frontières
Schaller,G., Scharer,D., Meynet, G., Maeder, A. 1992, A&AS, 96, 269
Soderblom D. R., Duncan D. K., Jonhson D. R., 1991, ApJ 375, 722
Soubiran C., 1994, Proc. IAU Symp. 161, "Astronomy from Wide Field Imaging", Potsdam, Germany, à paraître
Strömgren B., 1987, in *The Galaxy*, ed. Gilmore G. & Carswell, B., Reidel
Talbot R.J. & Arnett W.D., 1975, ApJ 197,551
Twarog B. A., 1980, ApJ 242, 242
Wielen R., 1974, in Hightlights of Astronomy, Vol. 4, ed. Contopoulos G., Dordrecht : Reidel
Wielen R., 1977, A&A , 60, 263
Wielen R., Jahreiss, H., & Krüger R., 1983, in *The Nearby Stars and the Stellar Luminosity Function*, IAU Coll. 76 eds. Philips D. & Upgren A. R.
Wood M. A., 1992, ApJ 386,539
Yuan J. W., 1993, A&A 261, 105

This article was processed by the author using Springer-Verlag LaTeX A&A style file *L-AA* version 3.